

# FSC 10214+4724: A GRAVITATIONALLY LENSED, HIDDEN QSO<sup>1</sup>

ROBERT W. GOODRICH,<sup>2</sup> JOSEPH S. MILLER, AND ANDRÉ MARTEL  
 UCO/Lick Observatory, University of California, Santa Cruz, Santa Cruz, CA 95064

AND

MARSHALL H. COHEN, HIEN D. TRAN, PATRICK M. OGLE, AND RENÉ C. VERMEULEN  
 Department of Astronomy, California Institute of Technology, Pasadena, CA 91125

Received 1995 July 31; accepted 1995 October 20

## ABSTRACT

We present polarimetric evidence that the extraordinarily luminous galaxy FSC 10214+4724 harbors a hidden QSO. In polarized flux we see broad emission lines of C III]  $\lambda$ 1909, C IV  $\lambda$ 1550, and Ly $\alpha$ /N V  $\lambda$ 1240. The narrow emission lines that dominate the total flux spectrum are unpolarized. Recent images have indicated that FSC 10214+4724 is actually gravitationally lensed, and we find strong evidence for Mg II  $\lambda$ 2800 absorption at  $z = 1.316$  in the spectrum of the QSO and weaker evidence for a possible continuum and absorption system at  $z = 0.893$ . Both of these systems could represent galaxies that contribute to the lensing.

*Subject headings:* polarization — quasars: absorption lines — quasars: general — quasars: individual (FSC 10214+4724)

## 1. INTRODUCTION

Among the ultraluminous galaxies discovered by *IRAS* is the unusual object FSC 10214+4724, reported by Rowan-Robinson et al. (1991) to be the most luminous object presently known. In addition to its large IR luminosity, FSC 10214+4724 produces intense CO emission, apparently indicating the presence of  $\sim 10^{11} M_{\odot}$  of molecular gas (Brown & Vanden Bout 1991; Solomon, Downes, & Radford 1992). With the discovery of high broadband polarization by Lawrence et al. (1993), it became apparent that the optical (rest-frame UV) light is predominantly scattered radiation, with the true source hidden from our direct view. In this sense it is similar to some high-redshift radio galaxies that also show high polarization rising into the UV, presumably from scattered light (e.g., Cimatti et al. 1993). High-resolution imaging of FSC 10214+4724 in the near-IR (Matthews et al. 1994; Graham & Liu 1995) and optical (Eisenhardt et al. 1996; Broadhurst & Lehár 1995) have shown an arc to the south of a round, resolved object. The morphology is suggestive of a partial Einstein ring, indicating that the great luminosity of FSC 10214+4724 derives in part from gravitational lensing (Elston et al. 1994). The spectrum of FSC 10214+4724 shows a wide range in ionization, which supports the idea that this object harbors an active nucleus (Elston et al. 1994; Soifer et al. 1995).

In the following work we present spectropolarimetry of FSC 10214+4724 with the intent of discovering the nature of the hidden energy source. The high signal-to-noise ratio (S/N) total flux spectrum that we obtain along with the polarization data also allows us to identify absorption lines that might be due to the lensing galaxy or galaxies.

## 2. OBSERVATIONS

FSC 10214+4724 was observed with the new imaging spectropolarimeter module of the Low-Resolution Imaging Spec-

trograph (LRIS; Oke et al. 1995) on the Keck telescope on 1994 November 6, November 7, and December 30. Exposure times on these respective dates were 900 s, 900 s, and 1050 s in each of four wave plate positions, and the slit position angles were at  $210^{\circ}$ ,  $260^{\circ}$ , and  $210^{\circ}$ , respectively, near the mean parallactic angles. A wavelength range of 3900–8900 Å was covered; the flux was corrected for slight contamination by the grating's second order using a simple model. A dispersion of  $2.5 \text{ Å pixel}^{-1}$  and a slit width of  $1''$  yielded a spectral resolution of  $9.4 \text{ Å}$  as determined from night sky and calibration lamp lines, or  $8.3 \text{ Å}$  as determined from features in the spectrum itself (see below). The seeing was  $\sim 0''.8$  during both runs.

Reduction to total flux and the two linear Stokes parameters ( $Q$ ,  $U$ ) followed standard techniques (e.g., Miller, Robinson, & Goodrich 1988). The wavelength scale was determined from observations of neon and argon lamps, and the zero point of the scale was fixed for each observation by measuring the centroid of the [O I]  $\lambda$ 5577 night sky line. The flux scale was determined from observations of spectrophotometric standards.

Emission and absorption lines in the spectrum of FSC 10214+4724 were measured using a Gaussian-fitting routine within the VISTA program and are reported in Table 1 in the observed frame. The formal uncertainty in the equivalent widths,  $W_{\lambda}$ , is  $\sim 0.2$ – $0.3 \text{ Å}$  for most lines. Many of the emission features in the rest-frame UV consist of two or more closely spaced components (e.g., N V  $\lambda$ 1240, Si IV  $\lambda$ 1402, C IV  $\lambda$ 1550, Al III  $\lambda$ 1860, C III]  $\lambda$ 1909), and in those cases multiple Gaussians were fitted with the separations fixed at the known wavelength differences of the components and the line widths identical in all components. This technique produces smaller line widths than those reported by Soifer et al. (1995), who fitted single Gaussians to each blend. We find the FWHM for the individual lines to be  $1260 \pm 140 \text{ km s}^{-1}$ . Our widths are consistent with those of Elston et al. (1994), except we find a higher N V  $\lambda$ 1240 width, in keeping with the other emission lines. The emission-line redshift is  $z = 2.2824 \pm 0.0001$ .

Note that narrow Ly $\alpha$  is quite weak compared to the other lines and appears double peaked. This is characteristic of

<sup>1</sup> Lick Obs. Bull. No. 1325.

<sup>2</sup> Present address: Space Telescope Science Institute, 3700 San Martin Drive, Baltimore, MD 21218.

TABLE 1  
LINE FLUXES IN FSC 10214+4724

Observed Wavelength	Observed Flux <sup>a</sup>	Observed $W_\lambda$ (Å)	ID	Rest Wavelength	FWHM (km s <sup>-1</sup> )
3982.0.....	1.84	28	Ly $\alpha$	1215.7	490
3986.5.....	1.72	27	Ly $\alpha$	1215.7	510
3999.9.....	2.1	32	Ly $\alpha$	1215.7	3,380
4073.0.....	9.5	183	N v	1240	1,230
4388.9.....	0.27	4.8	...	...	710
4599.1.....	2.9	66	Si iv	1400	1,415
4876.8.....	2.6	52	N iv]	1486.5	1,377
5085.9.....	12.9	253	C iv	1549	1,100
5256.3.....	0.8	16.5	[Ne iv]	1602	1,180
5384.5.....	6.40	124	He ii	1640.4	1,100
5464.9.....	0.4	8.6	O iii]	1664	1,290
5746.4.....	1.40	27	N iii]	1751	1,540
6126.2.....	0.18	3.4	Al iii	1856	...
6243.0.....	3.2	62	...	...	...
6264.9.....	3.8	74	C iii]	1908.7	1,120
6789.7.....	0.8	15.8	...	...	1,220
7041.3.....	0.6	11.7	N ii]	2142	1,380
7954.2.....	2.9	62	[Ne iv]	2422	1,130
8627.2.....	0.75	16.2	...	...	2,020
8632.4.....	0.14	3.0	...	...	290
5079.1 <sup>b</sup> ....	0.56	42	C iv	1550	6,000
6250.0 <sup>b</sup> ....	1.18	107	C iii]	1909	10,300

<sup>a</sup> Line flux in units of  $10^{-16}$  ergs cm<sup>-2</sup> s<sup>-1</sup>.

<sup>b</sup> Broad lines measured in Stokes flux,  $Q' \times F_\lambda$ .

resonantly scattered Ly $\alpha$ , as discussed by Bonilha et al. (1979) and Urbaniak & Wolfe (1981) among others. The expected position of Ly $\alpha$ , based on the other emission lines, is midway between the two peaks, as predicted. The separation of the peaks is 1.4 Å in the rest frame, half the value predicted by Urbaniak & Wolfe, and perhaps indicating an optical depth  $\sim 8$  times lower than they used in their models, or perhaps a different geometry. The red and blue peaks are the same height, indicating a small velocity gradient throughout the Ly $\alpha$  scattering region. The relative weakness of the entire line is likely due to dust absorption in the resonance-scattering region. Another possibility is that there is an absorbing cloud in front of the emission-line region that absorbs predominantly Ly $\alpha$ . This scenario seems a bit more ad hoc to us, since the absorbing cloud would have to have almost exactly zero velocity relative to the Ly $\alpha$  emission in order to produce such a symmetric resulting profile.

Our spectra did not fully resolve the north (N) and south (S) components of FSC 10214+4724, but we have tried to retrieve what spectral information we can from the fainter N component by using an iterative two-dimensional deblending technique on the 1994 December data set. At each wavelength in the two-dimensional spectral image, we first fitted two Gaussians, representing the strong S component (the arc) and the much weaker N component. We kept the width of the N Gaussian the same as that of the S Gaussian but left the other five parameters free. The FWHM value as a function of wavelength was then fitted with a straight line, and the Gaussian center of the S component fitted with a third-order polynomial. The average spatial separation between N and S Gaussians was measured to be  $1''.16 \pm 0''.03$ , consistent with the separation seen in images (Matthews et al. 1994; Graham & Liu 1995). Finally, a second pass was made through each image using these fits and allowing only the peak intensity of the two Gaussians to vary freely. In this way a spectrum of the N component was obtained with nearly optimal S/N and with

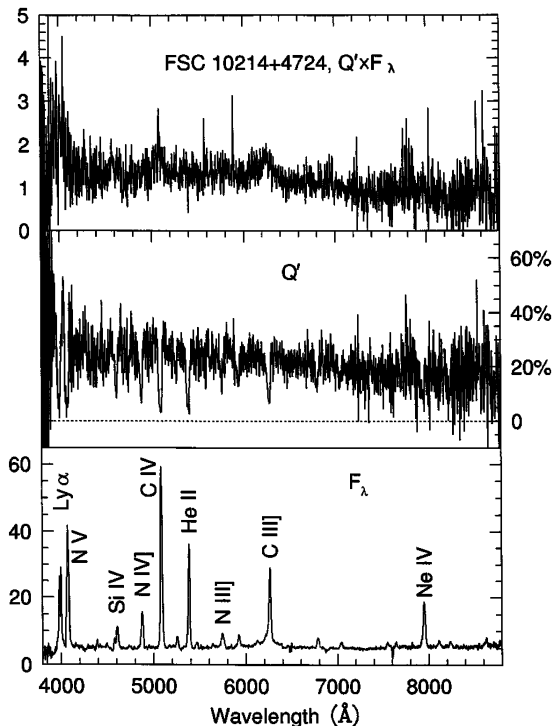


FIG. 1.—Spectropolarimetry data of FSC 10214+4724 are displayed from bottom to top as the total flux,  $F_\lambda$ , the rotated Stokes parameter (a measure of fractional polarization),  $Q'$ , and the Stokes flux (the polarized flux spectrum),  $Q' \times F_\lambda$ . Various emission lines are marked in  $F_\lambda$ . Note the lack of narrow emission lines in the Stokes flux and the presence of broad lines of C iii]  $\lambda 1909$ , C iv  $\lambda 1550$ , and Ly $\alpha$ /N v  $\lambda 1240$ . In this and subsequent figures,  $F_\lambda$  is in units of  $10^{-18}$  ergs cm<sup>-2</sup> s<sup>-1</sup> Å<sup>-1</sup>.

relatively little bias. Note that this spatial deblending technique was used *only to define the spectrum of the weak, N component*. Subsequent discussion of the spectra of the S component will refer to the standard reduction technique of summing over rows.

### 3. RESULTS

Figure 1 shows the spectropolarimetry of FSC 10214+4724. Since there is no evidence for a wavelength dependence of the polarization position angle, we use the mean value of  $\theta = 69^\circ 6 \pm 0^\circ 2$  to transform the observed Stokes parameters ( $Q$ ,  $U$ ) into the rotated Stokes parameter,  $Q'$ , shown in the middle panel, above the integrated flux,  $F_\lambda$ . The upper panel shows the “Stokes flux,”  $Q' \times F_\lambda$  (e.g., Goodrich & Miller 1995). A power-law fit to the Stokes flux gives a slope of  $\alpha = 1.4 \pm 0.3$  ( $F_\nu \propto \nu^{-\alpha}$ ). Note that Elston et al. (1994) required  $\alpha = 1.5$  to match the emission-line spectrum. An extrapolation of our power-law fit to  $1.65 \mu\text{m}$  yields  $Q' \times F_\lambda = 6 \times 10^{-19}$  ergs cm<sup>-2</sup> s<sup>-1</sup> Å<sup>-1</sup>, consistent with the upper limit of Elston et al.

In the polarization, represented by  $Q'$ , there are clear drops across the emission lines, consistent with zero polarization of the narrow lines. The Stokes flux represents the spectrum of the polarized component of light, and the absence of narrow emission lines in this spectrum further indicates that those lines are truly unpolarized. The continuum polarization shows a maximum at blue wavelengths [ $P(\lambda\lambda 4120\text{--}4200) = 26.5\% \pm 1.7\%$ ], dropping into the red [ $P(\lambda\lambda 7500\text{--}8000) = 15.9\% \pm 0.4\%$ ]. Our mean, flux-weighted continuum polarization from 4500 Å to 8000

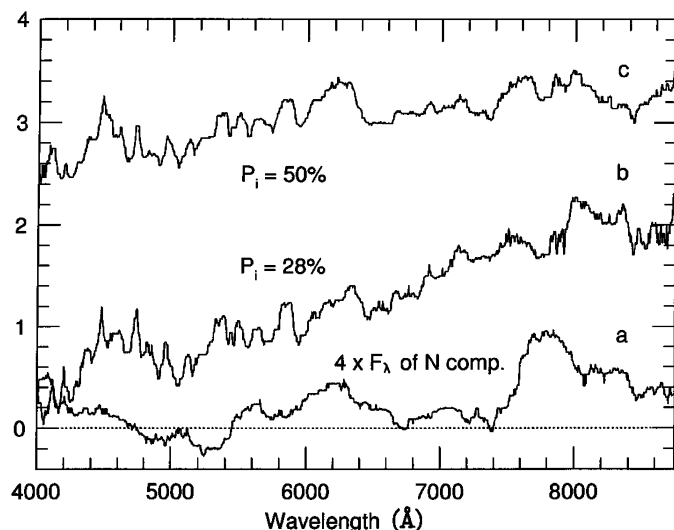


FIG. 2.—Spectrum of the N component (scaled by  $\times 4$ ) of FSC 10214+4724, which may be the lensing galaxy (or one of them), is shown by curve a. This curve has been smoothed using a median filter of 300 Å width (bar above spectrum). Note the possible continuum break at observed wavelength 7600 Å. Curves b and c are two possible shapes for the “unpolarized continuum” as described in the text (also smoothed by 300 Å). Curve b assumes an intrinsic polarization of the polarized spectrum of 28%, while curve c assumes 50%.

Å is  $P = 15.4\% \pm 0.1\%$ , consistent with previous measurements (Lawrence et al. 1993; Jannuzi et al. 1994).

Seen for the first time in the Stokes flux are broad components of Ly $\alpha$ /N v  $\lambda$ 1240, C iv  $\lambda$ 1550, and C iii]  $\lambda$ 1909. The broad-line parameters are given in Table 1. The equivalent widths,  $W_\lambda$ , are low for a QSO, indicating a high intrinsic luminosity (the Baldwin effect). Note that the broad component of C iii] is visible even in  $F_\lambda$ , although it is helpful to see broad C iii] in  $Q' \times F_\lambda$  in order to identify the line in  $F_\lambda$ . By assuming that the broad C iii] profile is the same in  $F_\lambda$  and  $Q' \times F_\lambda$ , we derive a broad-line polarization of  $P(\text{C iii])} = 30^{+20}_{-5}\%$ , the upper limit allowing some of the apparent flux in the broad wings of C iii] to be due to narrow emission lines from other ions. Similarly we find  $P(\text{C iv}) = 60^{+40}_{-10}\%$  for the broad C iv line. The ranges given are extreme values from eye estimates of the amount of wings in total flux and hence are not analogous to  $1\sigma$  errors but are comparable to  $2.5\text{--}3\sigma$  limits. Note that while  $P(\text{C iii])}$  is consistent with the continuum polarization,  $P(\text{C iv})$  appears to be significantly higher than  $P$  of the continuum.

The spectrum of the N component, derived as discussed in § 2, is shown, smoothed by 300 Å, in Figure 2. The S/N of the spectrum is low and precludes the detection of stellar absorption features, although a continuum break may occur near  $\lambda$ 7600. Possible slit losses will affect the overall flux level of the N component more than that of the brighter S component, as the slit was centered on the peak flux.

We also note the presence of a number of absorption features in the spectrum of the S component (Fig. 1). There are two broad features at  $\lambda$ 5520.4 and  $\lambda$ 6024.0. Two narrow, unresolved absorption lines<sup>3</sup> lie at 6477.1 Å and 6493.8 Å. The most likely identification for these is the Mg ii doublet

<sup>3</sup> The line widths are 8.3 Å, less than the widths of the neon lines used to wavelength-calibrate the spectrum. This is simply due to the fact that the neon lines fill the slit uniformly, while FSC 10214+4724 does not.

$\lambda_0$ 2796.35 and  $\lambda_0$ 2803.53 at a redshift  $z = 1.3163$ . The  $W_\lambda$  values of the lines,  $-2.8 \pm 0.2$  Å and  $-2.3 \pm 0.2$  Å respectively, imply hydrogen column depths of  $N_{\text{H}}$  greater than  $10^{18.3} \text{ cm}^{-2}$  and greater than  $10^{18.0} \text{ cm}^{-2}$ , respectively (Morton, York, & Jenkins 1988, assuming solar abundances).

We can use  $Q' \times F_\lambda$  and  $F_\lambda$  to attempt to derive an “unpolarized flux” (e.g., Trammell, Dinerstein, & Goodrich 1993). We assume that the intrinsic polarization of the continuum,  $P_i$ , is constant with wavelength. A second, unpolarized continuum is assumed to dilute the scattered light to produce the observed wavelength dependence of  $Q'(\lambda)$ . The shape of this unpolarized continuum is then  $F_\lambda - Q' \times F_\lambda / P_i$ . This continuum is shown in Figure 2 for two values of  $P_i$ , 28% and 50%. Note that it bears little resemblance to the derived spectrum of the N component on the same figure. This implies that either our assumption of constant  $P_i$  with wavelength is wrong or there is another source of unpolarized (or low-polarization) continuum in the spectrum of the arc itself (see below).

#### 4. DISCUSSION

The polarization spectrum of FSC 10214+4724 shows the broad lines typical of a QSO, similar to those seen in two other ultraluminous IRAS galaxies, IRAS 09104+4109 (Hines & Wills 1993) and FSC 15307+3252 (Hines et al. 1995). The high broad-line and continuum polarizations imply that the QSO is hidden from direct view, seen only in scattered light. The FWHM and  $W_\lambda$  of the broad lines in  $Q' \times F_\lambda$  are normal for QSOs.

An interesting feature of our data is that the polarization of the broad C iv line may be larger than that of the continuum. One explanation for this is that there is some other extended continuum source seen directly, perhaps analogous to the FC2 continuum deduced by Tran (1995) in Seyfert 2 galaxies. The spectral shapes b and c shown in Figure 2 could represent this FC2 component, under the assumption that the scattered light has a wavelength-independent polarization. The slopes of curves b and c are  $\alpha = 4.2 \pm 0.3$  and  $2.3 \pm 0.2$  ( $F_\nu \propto \nu^{-\alpha}$ ) for intrinsic continuum polarizations of 28% and 50%, respectively.

Broadhurst & Lehar (1995) show that in the B band the light is more dominated by the center of the arc than it is at K. Hence the arc center must represent a different spatial region than the ends of the arc, and this center is likely the main reflecting structure, or a part thereof. The redder ends of the arc could represent either the FC2 region (which in this picture is spatially separate from the reflection region) or another source of relatively redder continuum such as starlight. Broadhurst & Lehar argue that the region of the active galactic nucleus (AGN) that is highly magnified must be  $\sim 100 h^{-1} \text{ pc}$  in size, comparable to the reflection regions seen in some AGNs. Spatially resolved imaging polarimetry, perhaps with the *Hubble Space Telescope* (HST), will be important in clarifying the system's geometry.

The arclike morphology of FSC 10214+4724 indicates that it is likely to be lensed, quite probably by the N component, which is redder (Fig. 2) and is resolved in HST images (Eisenhardt et al. 1996). In our spectra we see three possible indications of the effects of the lens. First, the narrow Mg ii doublet seen in absorption at  $\lambda$ 6477.1, 6493.8 suggests the presence of a galaxy at  $z = 1.316$ . Weaker, but still possibly detected, absorption lines of Fe ii at this redshift lie at

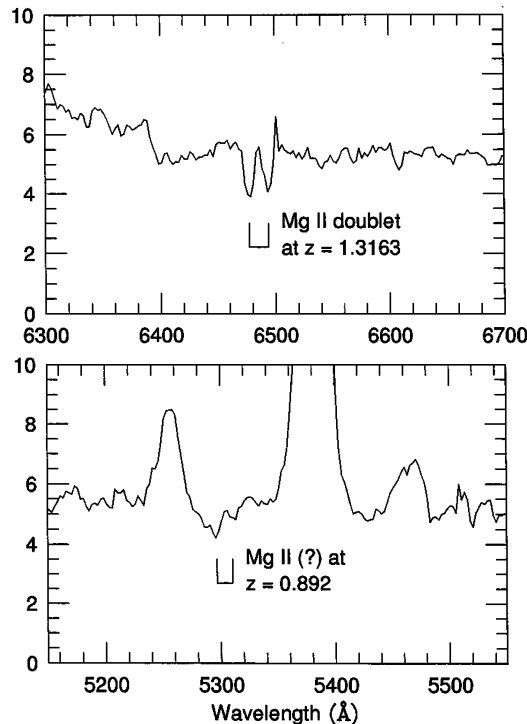


FIG. 3.—*Top*: The narrow absorption features from Fig. 1 which may be identified as a Mg II  $\lambda_0$ 2800 doublet from a galaxy at  $z = 1.3163$ . *Bottom*: The broad absorption feature which may represent a Mg II doublet at  $z = 0.893$ , consistent with continuum features seen in the N component, although this requires the doublet lines to have widths of  $970 \text{ km s}^{-1}$ . These absorption features may represent the foreground galaxy or galaxies responsible for the gravitational lensing of FSC 10214+4724.

$\lambda\lambda 6022.7, 5519.2$  ( $\lambda_0\lambda_0 2600.17, 2382.77$ ). Their detection in our spectra must be considered tentative, however. The continuum break in the spectrum of the N component at  $\lambda 7600$  (Fig. 2) could represent the  $4000 \text{ \AA}$  break common in galaxy spectra. In this case, the absorption feature at  $\lambda 5300$  (total  $W_\lambda = 5 \text{ \AA}$ ) could be the Mg II doublet at a redshift of  $z = 0.893$ , although the fitted line widths of  $970 \text{ km s}^{-1}$  are large for a galaxy. Serjeant et al. (1995) obtained spectra of the N component and a nearby object, estimating redshifts of  $0.896$  and  $0.899$ , respectively, from the continuum break near  $7600 \text{ \AA}$ . This provides additional support for the identification of this absorption system. The two absorption-line redshifts,  $z = 1.316$  and  $z = 0.893$ , could represent two galaxies along

the line of sight to the QSO, both of which contribute to the power of the gravitational lens. We have also searched for possible emission lines at these wavelengths, in particular [O II]  $\lambda_0 3727$ . A line at  $\lambda 8632.4$  in our spectrum could be [O II] at  $z = 1.316$ , although this part of the spectrum is noisy. At a redshift of  $z = 0.893$ , the [O II] line would fall on the red wing of the N II  $\lambda_0 2140$  line at the redshift of the background QSO, and while there is no evidence for the [O II] line there, the limit is not strong. In any case, it is not unusual for normal galaxies to show little or no [O II] emission.

Broadhurst & Lehar (1995) have demonstrated that gravitational lensing can explain the morphology of FSC 10214+4724. They, along with Trentham (1995), have also shown that the probability of such a lensing event in the *IRAS* sample is significant. Given the spectral shape of the N component (and a nearby galaxy; Serjeant et al. 1995) and the two sets of absorption features shown in Figure 3, our data raise the possibility of *two* foreground galaxies contributing to the lens power. This scenario has not been studied statistically yet. The N component has the colors expected for an elliptical galaxy at  $z = 0.893$ , and the more distant galaxy, at  $z = 1.316$ , is expected to be  $\sim 2$  mag fainter at  $8000 \text{ \AA}$ , due to the different  $K$ -correction involved.

Rowan-Robinson et al. (1991) originally identified FSC 10214+4724 as the most luminous known object in the universe. We now realize that its great luminosity derives in part from the amplification effects of a gravitational lens. Even so, FSC 10214+4724 is *one* of the most luminous objects known. With spectropolarimetry we have shown that it is a QSO, obscured from our direct view in the optical (rest-frame UV) but seen as its spectrum scatters off dust or electrons surrounding the QSO. The lensing galaxy or galaxies may be identified with the absorption lines seen in the spectrum of the QSO. Identification of counterimages and further modeling of the lens should provide significant constraints on the true luminosity of the QSO. Remaining to be determined are the amplification of the CO lines, the relative amplification of different regions of the nucleus, and the parameters of the lens itself.

The authors have benefited from discussions with L. Armus, T. Broadhurst, M. Dickinson, J. Graham, and T. Soifer. The referee also provided detailed and welcome comments. We also acknowledge the support of NSF grants AST88-18925 and AST91-21889. The W. M. Keck Observatory is operated as a scientific partnership between the California Institute of Technology and the University of California. It was made possible by the generous financial support of the W. M. Keck Foundation.

#### REFERENCES

- Bonilha, J. R. M., Ferch, R., Salpeter, E. E., Slater, G., & Noerdlinger, P. D. 1979, *ApJ*, 233, 649  
 Broadhurst, T., & Lehar, J. 1995, *ApJ*, 450, L41  
 Brown, R. L., & Vanden Bout, P. A. 1991, *AJ*, 102, 1956  
 Cimatti, A., di Serego Alighieri, S., Fosbury, R. A. E., Salvati, M., & Taylor, D. 1993, *MNRAS*, 264, 421  
 Eisenhardt, P., Armus, L., Hogg, D. H., Soifer, B. T., Neugebauer, G., & Werner, M. W. 1996, *ApJ*, in press  
 Elston, R., McCarthy, P. J., Eisenhardt, P., Dickinson, M., Spinrad, H., Januzzi, B. T., & Maloney, P. 1994, *AJ*, 107, 910  
 Goodrich, R. W., & Miller, J. S. 1995, *ApJ*, 448, L73  
 Graham, J. R., & Liu, M. C. 1995, *ApJ*, 449, L29  
 Hines, D. C., Schmidt, G. D., Smith, P. S., Cutri, R. D., & Low, F. J. 1995, *ApJ*, 450, L1  
 Hines, D. C., & Wills, B. J. 1993, *ApJ*, 415, 82  
 Januzzi, B. T., Elston, R., Schmidt, G. D., Smith, P. S., & Stockman, H. S. 1994, *ApJ*, 429, L49  
 Lawrence, A., et al. 1993, *MNRAS*, 260, 28  
 Matthews, K., et al. 1994, *ApJ*, 420, L13  
 Miller, J. S., Robinson, L. B., & Goodrich, R. W. 1988, in *Instrumentation for Ground-Based Astronomy*, ed. L. B. Robinson (New York: Springer), 159  
 Morton, D. C., York, D. G., & Jenkins, E. B. 1988, *ApJS*, 68, 449  
 Oke, J. B., et al. 1995, *PASP*, 107, 375  
 Osterbrock, D. E. 1989, *Astrophysics of Gaseous Nebulae and Active Galactic Nuclei* (Mill Valley: University Science Books)  
 Rowan-Robinson, M., et al. 1991, *Nature*, 351, 719  
 Serjeant, S., Lacy, M., Rawlings, S., King, L. J., & Clements, D. L. 1995, *MNRAS*, 276, 31  
 Soifer, B. T., Cohen, J. G., Armus, L., Matthews, K., Neugebauer, G., & Oke, J. B. 1995, *ApJ*, 443, L65  
 Solomon, P. M., Downes, D., & Radford, S. J. E. 1992, *ApJ*, 398, L28  
 Trammell, S. R., Dinerstein, H. L., & Goodrich, R. W. 1993, *ApJ*, 402, 249  
 Tran, H. D. 1995, *ApJ*, 440, 597  
 Trentham, N. 1995, *MNRAS*, submitted  
 Urbaniak, J. J., & Wolfe, A. M. 1981, *ApJ*, 244, 406